Investigating the use of 3D laser scanning to detect damage features in heritage buildings

Antón, Daniel * *danton@us.es*

PhD, MSc, BSc, HNC

(1) Departamento de Expresión Gráfica e Ingeniería en la Edificación, Escuela Técnica Superior de Ingeniería de Edificación, Universidad de Sevilla, Seville 41012, Spain

(2) Researcher, The Creative and Virtual Technologies Research Lab & Product Innovation Centre, School of Architecture, Design and the Built Environment, Nottingham Trent University, Nottingham NG1 4FQ, United Kingdom

Amaro-Mellado, José -Lázaro

(3) Departamento de Ingeniería Gráfica, Universidad de Sevilla, Seville 41092, Spain

Al-Habaibeh, Amin

(4) Product Innovation Centre, School of Architecture, Design and the Built Environment, Nottingham Trent University, Nottingham NG1 4FQ, United Kingdom

Abstract

Terrestrial Laser Scanning (TLS) is becoming increasingly important in the cultural heritage field given the need for virtual records of buildings and detecting surface wear and deterioration. Scientific research has shown that exhaustive 3D modelling from point clouds enables accurate analysis of heritage buildings and sites. However, factors such as the number and location of scanning stations, distance to objects, point of view, and resolution impact the scanning and modelling accuracies. Through the case study of a 19th-century Anglican masonry church in Nottingham (UK), this chapter investigates the accuracy of TLS surveying features to model surface deficiencies in heritage buildings. The results showed that combining different points of view and distances can enhance accuracy, but the joint accuracy is still lower than that of the less unfavourable station. The research also determined the suitable meshing smoothening for damage modelling and analysed the point cloud discretisation distortion for accuracy analysis.

Keywords: Terrestrial laser scanning; 3D point cloud data; model accuracy; damage; heritage; point cloud; accuracy; 3D modeling; as-built; 3D scanning; point cloud data; HBIM; CAD; computer-aided design; 3D mesh; computer graphics; pathology; pathologies; building; heritage site; historic building; heritage asset

1. Introduction

The UNESCO World Heritage Convention (United Nations Educational Scientific and Cultural Organization (UNESCO), 1972) stressed the uniqueness and need to protect heritage, the valuable and irreplaceable legacy from the past of all the peoples of the world (United Nations Educational Scientific and Cultural Organization, 2019). For heritage to prevail in this rapid-developing world, continuous maintenance and conservation actions must take place. To this end, the Athens and Venice Charters (International Council on Monuments and Sites,

2011)(International Council on Monuments and Sites, 2004) promoted the use of modern techniques and materials in the restoration, the process of returning heritage assets to their original condition and/or spatial layout, but also consolidating them to be durable over time, thus retaining their historic integrity. To support this, digital tools have been implemented in such a way that heritage assets can be studied, understood, and virtually reconstructed from documentary sources.

1.1. 3D scanning in Cultural Heritage

In recent years, as indicated by Li et al. (Li et al., 2023), the current practice of built heritage protection is constantly based on three-dimensional LiDAR, which accounts for light detection and ranging. 3D LiDAR, which operates in an analogous way to radar, is an active sensor that records surrounding 3D information (Huang et al., 2022). As described by Huang et al. (Huang et al., 2022) this technology obtains the distance of target bodies by illuminating laser signals (pulses) at specific wavelengths on those targets. This is performed using the time-of-flight (ToF) principle, which modulates laser beams over time. In other words, the emitter of the device shoots a laser pulse at the target body, and the receiver collects the reflected laser pulse. The ToF method measures the round-trip flight time of emitted laser pulses to determine the distance between the LiDAR device and the target. This, carried out throughout the target surface, captures 3D point cloud data (spatial data in XYZ coordinates).

The use of 3D scanning technology has been extensively investigated to detect damage in heritage buildings in high resolution. In other words, it provides detailed insight into the real state of conservation and the behaviour of the assets in order to generate new knowledge for their life cycle. This technology produces highly accurate qualitative and quantitative information that can be used to assess complex structures under a non-destructive and efficient approach, thus supporting restoration actions for the conservation of architectural and cultural heritage. Particularly, Terrestrial Laser Scanning (TLS) can be used to detect and monitor surface deficiencies in heritage buildings (Antón et al., 2022) using both 3D point clouds and their laser intensity data (TLS radiometric data; Red, Green, and Blue (RGB) values depending on the reflection of the laser beam on surfaces). Combined with unsupervised classification methods for digital image processing, TLS intensity data is also useful for the detection of damage deriving from moisture content in stone materials of historic buildings (Armesto-González et al., 2010). Likewise, other researchers (Lezzerini et al., 2016) used computer-aided design (CAD) and Geographic Information System (GIS) software to map different stone materials of the medieval Church of St. Nicholas in Pisa, Italy, using TLS data, high-resolution images, and organoleptic data of the building surface. As a result, the façade of that historic building was characterised in terms of materials, stages, and techniques used to build it. Regarding the virtual representation of geometrical alterations for heritage buildings and archaeological sites, TLS has been used as the data source to develop semi-automatic as-built or as-is 3D modelling approaches (Antón et al., 2018)(Antón et al., 2019) compatible with Historic Building Information Models (HBIM). In this way, 3D meshing algorithms and visual programming language implemented in CAD software packages can be used to model both structural and surface irregularities and singularities of the assets. Consequently, the recording of surfaces using this remote sensing technique can be further applied to the early detection and monitoring of the damage and changes in historic building surfaces, i.e., their surface wear and deterioration and their evolution over time. This is the case of the research by Dawson et al. (Dawson et al., 2022), who monitored and detected minor changes in a historic site thanks to TLS surveys in the long term. Similarly, Lercari (Lercari,

2019) conducted multi-temporal TLS monitoring and surface change detection at the millimetric scale from the resulting 3D point clouds of Neolithic earthen structures.

As seen above, the scientific community has embraced TLS because of its great capabilities. In particular, it can be used in developing countries to digitise heritage buildings and sites that are endangered (United Nations Educational Scientific and Cultural Organization (UNESCO), 2023a). The threats include natural disasters, climate change and agents, the expansion of urban areas, pollution, war, uncontrolled tourism (United Nations Educational Scientific and Cultural Organization (UNESCO), 2023b), and other human activities and behaviours such as vandalism. Besides, TLS can be combined with many other technologies to:

- Provide a more comprehensive and integrated approach to studying heritage buildings and sites for conservation: The physical and spatial characteristics of the heritage assets can be analysed alongside their information when using 3D point cloud data on Building Information Modelling (BIM) platforms and GIS (Geographic Information Systems). Moyano et al. (Moyano et al., 2021) experimented with HBIM parameterisation through semantic segmentation applied to a TLS point cloud dataset of one of the façades of a heritage building in Seville, Spain. Klapa et al. (Klapa & Gawronek, 2022) studied the synergies between TLS and UAVs (unmanned aerial vehicles) for the creation of HBIM, in which the authors placed greater importance on the accuracy of the measurement information than on the selection of the level of detail itself. Still, HBIM open-source technology is a cutting-edge topic, and an extensive review can be found in the research paper by Diara (Diara, 2022). Haznedar et al. (Haznedar et al., 2023) proposed a workflow for 3D point cloud segmentation for heritage buildings using deep learning by implementing PointNet, thus improving the HBIM capabilities. Regarding GIS, Campiani et al. (Campiani et al., 2019) inserted deterioration—calculated by comparing TLS data in different periods—and environmental values of earthen walls in a Neolithic site into a GIS to relocate conservation interventions to more urgent areas. Doğan and Yakar (Doğan & Yakar, 2018) developed a GIS to integrate and document 3D data for cultural assets in Turkey. Pepe et al. (Pepe et al., 2021) employed a Scan-to-BIM method for heritage assets in order to create a 3D GIS model that enabled a multidisciplinary view. This was conducted by integrating TLS and close-range photogrammetry, and a BIM project was loaded into a 3D GIS, thus facilitating multiple information connections.
- Significantly improve the efficiency and accuracy of damage detection in heritage buildings: Yang et al. (Yang et al., 2023) reviewed the use of non-artificial intelligence-based algorithms to perform 3D point cloud segmentation of cultural heritage datasets, and machine learning and deep learning methods to conduct semantic segmentation. Thanks to these approaches, damage detection can be automated. Nevertheless, those authors indicated that, among other issues, these methods are mainly limited to historic buildings, suffer from over-segmentation, lack consistency when processing data from multiple sources, and should improve for larger datasets, although progress is being made in large-scale scene segmentation (Liao et al., 2022). Dayal et al. (Dayal et al., 2019) also analysed damage detection of heritage monuments from TLS point clouds an terrestrial optical data in India. To this end, the authors converted the 3D point cloud into a 2D dataset, leading to an “unrolled” point cloud that was employed to generate raster images. They undertook the damage detection through an approach based on geometry and a radiometric data. Alkadri et al. (Alkadri et al., 2022) examined surface fractures and material behaviour from TLS point cloud attribute information for a church in Java, Indonesia.

- Improve the processing and analysis of massive TLS datasets, i.e., a substantial number of points in space: Research (Pajić et al., 2018)(Liu & Boehm, 2015) has addressed the management of large-scale 3D point clouds in a big data context for processing and semantic classification. Other authors (Nguyen et al., 2022) researched a cost-effective and user-friendly large point cloud rendering solution based on a potential distributed computing framework for big data storing and processing (Hadoop) for distributed computing applications in civil engineering, including progress monitoring, change detection or indoor navigation. Compared to conventional solutions, they achieved improved performance, scalability, and fault tolerance. Duchnowski and Wyszkowska (Duchnowski & Wyszkowska, 2022) modelled vertical terrain displacement from massive TLS data using M_{split} estimation, which the authors proved to be more accurate than least-square or robust M-estimation.
- Make 3D scan data of historic buildings and sites more accessible and user-friendly, especially for non-expert users, to support the dissemination and conservation of heritage assets. This can be done by importing 3D point cloud data into immersive technologies such as augmented reality (AR), mixed reality (MR), and virtual reality (VR). Thus, Patel et al. (Patel et al., 2021) explored the methodology of bridge inspection from TLS and AR, mainly to cover unreachable spots, from the office, not from the site. Janeras et al. (Janeras et al., 2022) employed MR to display and distribute 3D data of the Montserrat Massif (Spain) during a stability assessment, leading to better risk communication to the users. Finally, Poux et al. (Poux et al., 2020) designed a system to implement a VR application for multidisciplinary users, which was tested in a Belgium castle from a TLS 3D point cloud.

1.2. Limitations of TLS

In spite of the numerous benefits of TLS and future advances and its combination with other diverse technologies, this remote sensing technique is not free of limitations or challenges. These issues can be divided into two different groups:

Financial

- Even if the purchase of state-of-the-art devices is not considered, 3D scanning equipment can be expensive, especially when high resolution and accuracy are needed. According to Disney et al. (Disney et al., 2019), TLS instruments over $100,000 are beyond the reach of most researchers. In contrast, low-cost devices are in the region of $20,000, which is still a significant amount of money for many users. For those cases, the Structure-from-Motion (SfM) photogrammetric technique is the very low-cost alternative, for which the only requirement for data collection is access to a camera. Furthermore, handling and processing massive 3D point cloud data requires high-performance workstations and/or laptops.

Operational

- Time-related: Especially for large and complex heritage buildings and sites that require hundreds of stations (scan positions), TLS surveying can be a time-consuming process, although there are few other options currently available. The time that the fieldwork takes does not only depend on the (scan and image) recording period but also on the survey planning, the levelling of the tripod, and the recording of targets for subsequent

registration. In addition, as seen in the work by Julin et al. (Julin et al., 2020), TLS imaging quality also influences the total data acquisition time spent in the field since the performance of the equipment significantly differs when choosing Low Dynamic Range (LDR) or High Dynamic Range (HDR) imaging. Finally, the processing and analysis of 3D point cloud data may require spending considerable time depending on the computer specifications, the number of stations and points recorded, the resolution and other parameters set in the TLS survey, the intended point density, the segmentation and cleaning of the data, among many others, with a view to extracting meaningful information.

- Image quality: Research has found poor colourisation of 3D point clouds depending on which TLS device is used (Julin et al., 2020), and their image quality is far inferior to what can be achieved by SfM photogrammetry. As explained by Julin et al. (Julin et al., 2020), low image quality has an impact on the direct applicability of coloured 3D point clouds to diverse cases that need to rely on visual appearance or radiometric values for object interpretation and recognition, visual analysis, or photorealism. Those authors considered that enhanced colouring of 3D point cloud data would be relevant and useful for traditional application areas. These domains cover engineering, surveying, or cultural heritage but also emerging application fields such as virtual production in the film industry or the creation of 3D content for video games and immersive experiences.
- Accuracy: The accuracy of the 3D recording depends on numerous factors. Firstly, it depends on the TLS device used. Here, as seen in the work by Chen et al. (Chen et al., 2018), the ability of the LiDAR sensor to measure both time and the laser beam width has an impact on the recording accuracy. Secondly, the accuracy of 3D scanning results depends on several factors such as illuminance and atmospheric conditions, surface characteristics of the building (materials, moisture content, dust, among others), number and location of stations, distance to the object, point of view, and resolution. These aspects also influence the intensity of the point cloud data, as the laser beam incidence angles and distances may differ.

With a special focus on accuracy, the scientific community has studied the effect of TLS parameters on crack width measurement in different materials and damage sizes. Nevertheless, the quantification of depth recording errors still needs to be addressed, especially in hybrid materials (Oytun & Atasoy, 2022). For their part, other researchers (Tan & Cheng, 2017) investigated the effects of specular reflection on the accuracy of the scan data. They corrected the incidence angle to eliminate the specular reflection effects for TLS intensity image interpretation and 3D point cloud representation by intensity. The authors explained that scanning at larger incidence angles avoids the influence of specular reflection effects in the intensity data of smooth surfaces. Consequently, perpendicular scanning should be avoided, as in the case of a different remote sensing technology, infrared thermography, where the camera operators themselves constitute a source of emissions that must be taken into account (Antón & Amaro-Mellado, 2021). However, as indicated by (Soudarissanane et al., 2011), increasing incidence angles implies higher measurement errors, i.e., lower quality in point clouds. Finally, Tan et al. (Tan et al., 2018) studied anomalous distance measurement errors caused by target specular reflections. Their results revealed that distance measurement errors are strongly related to the original intensity values, so the correction of those errors leads to significantly improved accuracy.

In view of all the above limitations and determining factors of TLS surveys, this chapter aims to investigate the accuracy and precision of 3D laser scanning positioning to detect damage

features of heritage buildings and how to enhance detection and monitoring for their preservation over time.

The rest of this chapter is organised as follows: Section 2 describes the case study that will be used in the investigation, details on the TLS survey, processes to carry out the geometry and accuracy analyses on 3D point clouds and meshes, and the specifications of the equipment used for data processing and analysis. Section 3 presents the results and their discussion, as well as the limitations of the research. The conclusions and future work are described in Section 4.

2. Methodology

This research investigates TLS survey accuracies and positioning for the recording of surface damages in heritage buildings. Hence, it is worth describing the selected case study for that purpose.

2.1. Case study: St John the Baptist Church in Nottingham, UK

This research is developed through the case study of the Church of St John the Baptist, also called Beeston Parish Church, an Anglican temple in Beeston, Borough of Broxtowe, in the city of Nottingham (Nottinghamshire County, East Midlands region in England, the United Kingdom). The site map with coordinates is shown in Figure 1.

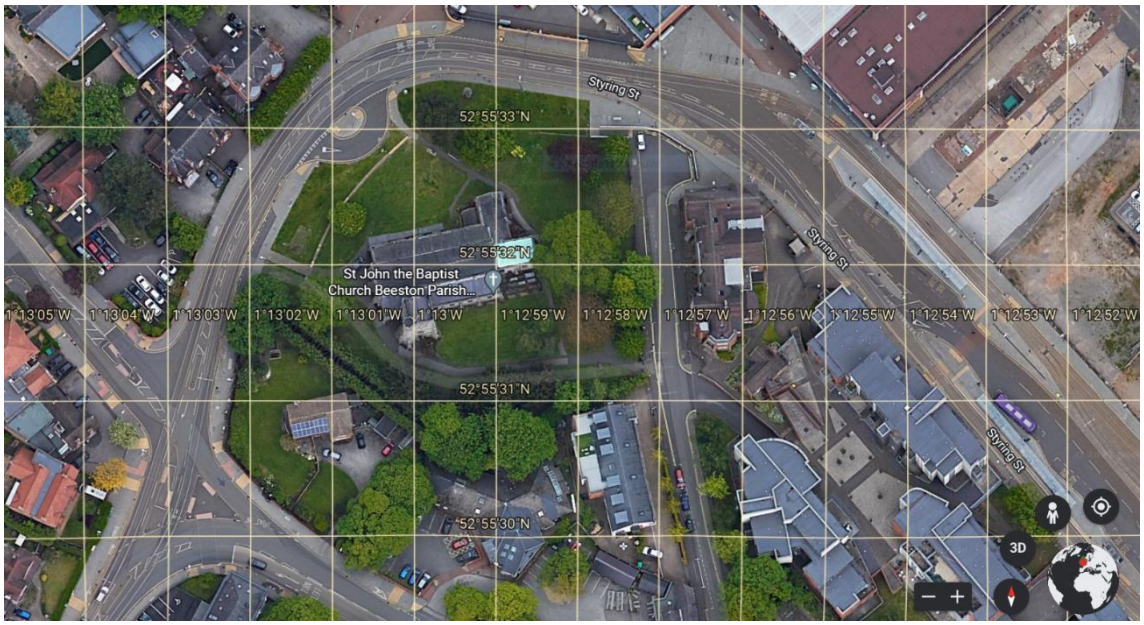

Figure 1. Site map of St John the Baptist Parish Church with coordinates. Source: Google Earth with 2D satellite imagery.

The Church of St John the Baptist was listed as a Grade II historic building by Historic England (Historic England, 1987) with List Entry Number: 1263823 (it was formerly listed 18.lO.49 as Parish Church of St John). This temple dates from the mid-19th century; since then, restoration interventions have taken place on its tower and bells, roofs, and interior walls (The Southwell and Nottingham Church History Project, 2021). This heritage building presents diverse surface pathologies such as patina of lichen and moss, moisture, and stone mass loss in masonry blocks. The latter is the case of a section of a wall of approximately 1.65 m (width) x 1.95 m (height)

oriented to the West, with damaged blocks scattered on it, mainly in the bottom and at mid-height. The target wall is indicated in Figures 2 and 4.

Figure 2. St John the Baptist Parish Church. North façade and target wall. Source: The authors, based on Google Street View.

2.2. 3D laser scanning

In order to study the TLS measurements on the aforementioned wall, a comprehensive 3D survey was first carried out throughout the exterior and interior of the building. However, the interior was not considered in this research as it was beyond its scope. The geometry of the temple was recorded using a tripod-mounted Leica Geosystems ScanStation P20 3D laser scanner (Leica Geosystems, 2012), as can be seen in Figure 3. The survey parameters were as follows: the resolution was set at 6.3 mm at 10 metres and 3.1 mm for closer and further stations, respectively; full scanning range and horizontal and vertical angles were established; and HDR imaging was selected.

Figure 3. St John the Baptist Beeston Parish Church and the 3D laser scanner. Wide-lens Southeast perspective. Source: The authors.

The TLS survey was carried out according to previous planning consisting of a total of 17 stations surrounding the building. No targets were placed outside the temple given the sufficient overlap (enough points) between scans.

2.2.1. Registration diagnostics

Leica Cyclone 9.4 (Leica Geosystems, 2019) was used to process the scan data after collection. This allowed for creating constraints between the clouds so that the stations were registered, i.e., aligned in the same coordinate system. This process was mainly automatic because of the overlap described above. However, given the numerous trees surrounding the building, the algorithm may have had difficulties registering the scans. As a result, certain scan links (constraints) needed the manual selection of three pairs of common points between the datasets for accurate alignment, which was further optimised by using the automatic tool in Cyclone. Next, the programme was also used to generate the alignment report (registration diagnostics, Table 1), which consisted of essential data to certify and understand the accuracy of the process. In addition to specifying the stations matched, the strength of the scan links, the overlapping points, and the average errors, the report included the Root Mean Square Error (RMSE) of each constraint as per equation (1) (Xu et al., 2021).

$$RMSE = \sqrt{\frac{1}{N}\sum_{i=1}^{N}\left\|p_i - q_j\right\|^2}, (1 \le j \le M), \quad (1)$$

where p_i and q_j are, respectively, the nearest corresponding pair of points in clouds *P* and *Q,* and *N* and *M* account for the registration scales of those clouds.

Table 1. Registration diagnostics of the exterior TLS survey of Beeston Parish Church. Source: The authors.

Constraint ID	Station no.	With station no.	Weight (coefficient)	Overlap (points)	Average error (m)	RMSE (m)
1	6	16	0.9218	714,800	0.003	0.023
2	7	16	0.8251	332,366	0.003	0.028
3	13	14	1.0000	319,433	0.001	0.019
4	1	2	1.0000	885,066	0.003	0.024
5	8	9	0.7213	335,033	0.001	0.026
6	3	4	1.0000	885,966	0.002	0.021
7	5	6	0.5751	487,066	0.004	0.018
8	3	15	0.7300	622,200	0.002	0.021
9	7	8	0.5048	116,033	0.002	0.029
10	15	17	0.6369	901,700	0.001	0.021
11	8	10	0.4648	214,800	0.001	0.025
12	5	7	0.4453	169,700	0.004	0.024
13	4	5	0.5345	608,433	0.001	0.018
14	6	7	0.3883	216,366	0.002	0.025

15	9	10	0.3485	463,833	0.001	0.021
16	3	5	0.4384	658,800	0.003	0.022
17	10	11	0.1964	549,266	0.004	0.022
18	1	13	1.0000	243,700	0.001	0.024
19	1	14	1.0000	319,966	0.001	0.023
20	2	3	1.0000	525,933	0.002	0.021
21	2	4	1.0000	435,766	0.001	0.021
22	2	14	1.0000	319,666	0.002	0.025
23	9	11	1.0000	513,400	0.002	0.025
24	11	12	1.0000	479,366	0.001	0.025
25	12	13	1.0000	477,533	0.001	0.025
26	12	14	1.0000	324,833	0.001	0.027

The mean absolute error of the TLS survey registration was only 0.002 m (two millimetres). In relation to the RMSE, the lower it is, the better the registration result.

2.3. Geometric and accuracy analysis

2.3.1. Assessing the TLS survey layout

Once the details of the alignment have been presented, it is worth showing the selected stations to be used to assess the accuracy of the damage recording on the target wall. To do this, this research took into account the findings of Tan and Cheng (Tan & Cheng, 2017) to avoid specular reflection effects in 3D point cloud intensity data by scanning at greater angles and avoiding perpendicular recording, at least over short distances. At the same time, consideration was given to what Soudarissanane et al. (Soudarissanane et al., 2011) reported on the occurrence of higher measurement errors at large angles of incidence, thus entailing lower quality in point clouds. The layout of the stations also depended on the planned positions of the scanner to avoid occlusions affecting the TLS recording of the entire exterior of the church.

6 out of the 17 stations of the Beeston Parish Church TLS survey captured the geometry of the target wall. However, considering the above criteria, two stations were discarded for excessive incidence angle and occlusions. Therefore, four stations were chosen to analyse the accuracy of the recording and damage detection on the heritage building. From the arrangement of these four remaining stations, two of them were selected as the ground truth for the analysis (stations 17 and 15). They were the closest to the target wall (A and B, respectively, in Figure 4 and Tables 2 and 3), thus providing the highest resolution in the 3D point cloud and a low average error (1 mm). These stations also faced the target wall from each side.

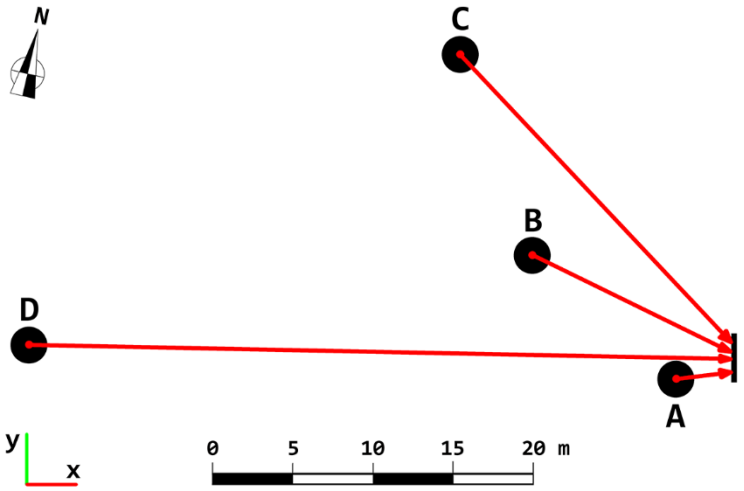

Figure 4. Layout of selected stations for accuracy analysis, and target wall (right). Top view. Source: The authors.

To ease understanding, a letter was given to each station from the registration diagnostics list depending on their distance to the target wall (please see Table 1 and Figure 4 above, and Table 2).

Table 2. Reader-friendly naming of scan stations. Source: The authors.

Station ID	17	15	3	1
Station name	A	B	C	D

Table 3. Distance from stations to target, approximate incidence angle, scanning resolution, and measured wall target cloud resolution. Source: The authors.

Station name	A	B	C	D
Mean distance to target (m)	3.85	14.15	25.50	43.95
Incidence angle (°)	70	63	42	89
Scanning resolution at 10 metres (mm)	6.3	3.1	3.1	3.1
Point resolution in wall target cloud (mm)	< 3	< 5	< 8	< 14

2.3.2. Accuracy analysis

To analyse the recorded surface at each station, a previous segmentation process was needed to extract the target wall from the 3D point cloud. This also allowed for the removal of noise and unwanted sectors. Open-source software such as CloudCompare (Girardeau-Montaut, 2016) permits the manual creation of polygon fences to enclose the desired points and then compute the trimming.

As described above, the geometry of reference (ground truth) consisted of point cloud data of the target wall from stations A and B (1 mm average error in the alignment; please see Table 1). Therefore, it is worth analysing the accuracy of stations C and D to assess the suitability of different points of view for the detection of damage on heritage building surfaces.

Point deviation analysis

The Cloud-to-Cloud (C2C) Distance computing tool (Girardeau-Montaut, 2015a) in CloudCompare software enables point deviation measurements to be conducted between two point clouds. In addition to a histogram of the distance between them, statistical data such as mean distance and standard deviation are also provided to offer insight into the scanning accuracy. This was useful to compare the clouds from stations C and D against the reference cloud to assess their accuracies, but also if combining the point clouds from those two unfavourable stations (due to excessive distance and incidence angle) significantly improves the accuracy of the scanning. The results will be shown in section 3.

Accuracy of damage modelling: 3D meshing

The scientific community has demonstrated that TLS data is useful in capturing heritage building surface deficiencies. However, 3D modelling constitutes a step forward towards further analysis and simulation. 3D meshes (triangle-based 3D objects) and 3D solid models of heritage assets in CAD and BIM environments have been used for virtual reconstruction and studies to contribute to their conservation and dissemination. For these reasons, the accuracy analysis of 3D meshing should be addressed to ensure surface defects in historic buildings can be represented. In this sense, this research focuses on the following accuracy indicators:

a) Different smoothening degrees in the 3D meshing of the reference geometry (target wall cloud from stations AB, ground truth in the analysis) should be analysed and compared with each other to find the optimal smoothening degree to model surface deficiencies in the heritage building.
b) The accuracy of clouds of the target wall from stations A and B should be verified against the reference cloud and optimal mesh (AB) to find the most suitable TLS parameters in the survey. This was carried out by running the C2C tool and the Cloud-to-Mesh Distance computing tool (Girardeau-Montaut, 2015b) in CloudCompare software, which enables point deviation measurements to be conducted between a point cloud and a mesh, or those of two meshes with each other, although the vertices of one of them will be chosen instead the mesh itself.
c) Finally, it is worth analysing the accuracy of each component of the ground truth point cloud data, A and B, against the reference 3D mesh (AB) in order to calculate the distortion from discretising their geometry.

3D meshes were generated from the selected 3D point clouds using a plug-in in CloudCompare based on the Screened Poisson Surface Reconstruction algorithm developed by Kazhdan and Hoppe (Kazhdan & Hoppe, 2013). This requires that the point sets have their normal vectors calculated. Once this was conducted, the smoothening degree was determined by selecting the Octree depth value (level). Qualitative testing indicated that levels 9 and 10 enabled the representation of surface defects on the target wall without excessive simplification (loss of deformation details) or number of triangles (larger file size), respectively. As a consequence, both levels needed to be analysed to determine the optimal smoothening degree for accuracy analysis through cloud-to-mesh and mesh-to-mesh distance computations.

When creating an open surface that extends beyond the point cloud edges (Neumann meshing method), it is necessary to segment the excess part so that its vertexes are not taken into account in the accuracy analysis. This was carried out by filtering mesh vertexes by the desired density values, so that outliers that were not part of the target wall geometry were removed.

To do this, it was possible to set the 3D mesh density as scalar field values thanks to the aforementioned CloudCompare plug-in.

2.4. Equipment used

As seen in previous sections, the TLS equipment consisted of a Leica Geosystems ScanStation P20 3D laser scanner. The computer used to process and 3D mesh the 3D point cloud data and perform the analysis was a high-performance gaming laptop with an octa-core processor with hyper-threading at 2.30 GHz and a maximum turbo frequency of 4.60 GHz with 24 MB cache, 32 GB RAM DDR4 @ 3200 MHz, a 256-bit graphics card with 6144 cores @ 1245 to 1710 MHz and 8 GB GDDR6 dedicated memory @ 14 Gbps, and a 1TB NVMe PCIe Gen3x4 SSD (solid-state drive).

3. Results and discussion

This section aims to gather, interpret and examine the outcomes of the accuracy analysis on 3D point clouds of each TLS survey station and the 3D meshes of the surface deficiencies detected on the target wall of the case study. This includes analysing the point deviation of station clouds that derive from their incidence angle, resolution, and distance to the target against the ground truth, the reference dataset resulting from the combination of two accurate stations (A and B) for presenting more favourable surveying features.

3.1. Suitability of TLS surveying characteristics for damage detection on heritage buildings

This sub-section addresses the accuracies of both 3D point clouds and meshes by applying the approaches described in the methodology.

3.1.1. Accuracies of station clouds

Qualitatively speaking, special mention should be made of the evident difference in resolution between the 3D point cloud data from stations D and C, and the ground truth (AB) (please see Figure 5 below). There is a greater distance between points in the former stations in comparison with the dense cloud in the more accurate cloud AB (right). Here, in the reference stations, shorter distances to the target wall and increased resolution set before scanning made the difference. This can also be seen in Table 3 with quantitative data. Considering this table, station C implied a greater incidence angle of the laser beam on the target wall, whose implications in mean distance between clouds and point accuracy (standard deviation value) will be shown below. Figure 5 shows the two compared stations and the reference cloud, which is much more detailed. Because of the greater angle in station C (centre), the points are not arranged in a quasi-regular grid as in station D (left). This entails lower accuracy in cloud C in comparison with a hypothetical station established at the same distance as C but with a lower angle (closer to perpendicularity) to the target wall.

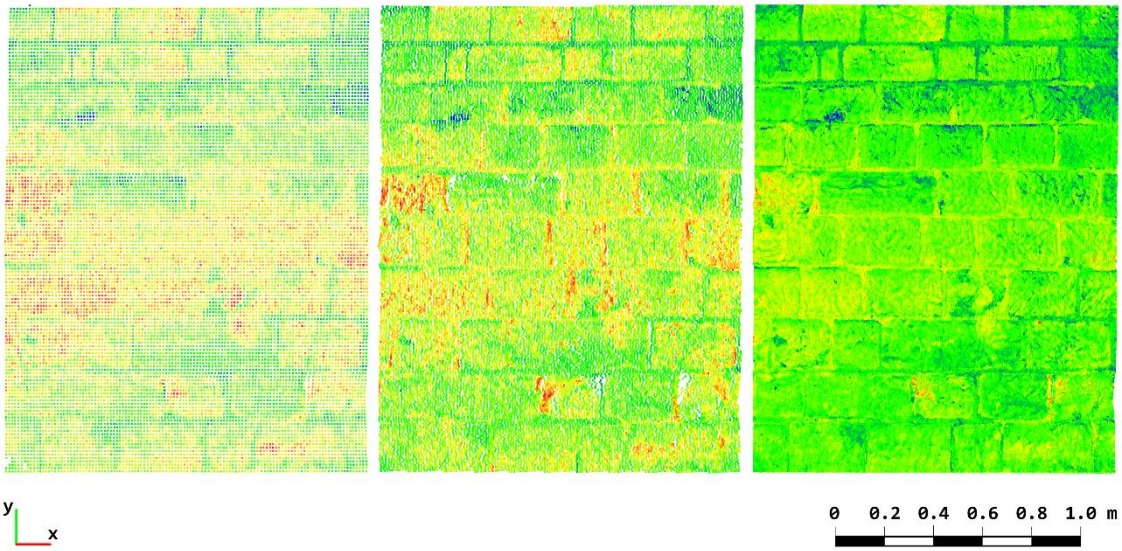

Figure 5. Target wall clouds from stations D (left), C (centre), and the ground truth AB (right). Rainbow colour gradient for intensity visualisation. Elevation view. Source: The authors.

The C2C Distance tool in CloudCompare yielded the following data from the point deviation analysis in clouds:

Station D against the ground truth (AB)

These are the results of the accuracy analysis of the most distant station with the most perpendicular angle and the reference cloud:

Mean distance = 0.004341 metres

Standard deviation = 0.001952 metres

The histogram of absolute point distances is shown in Figure 6 below.

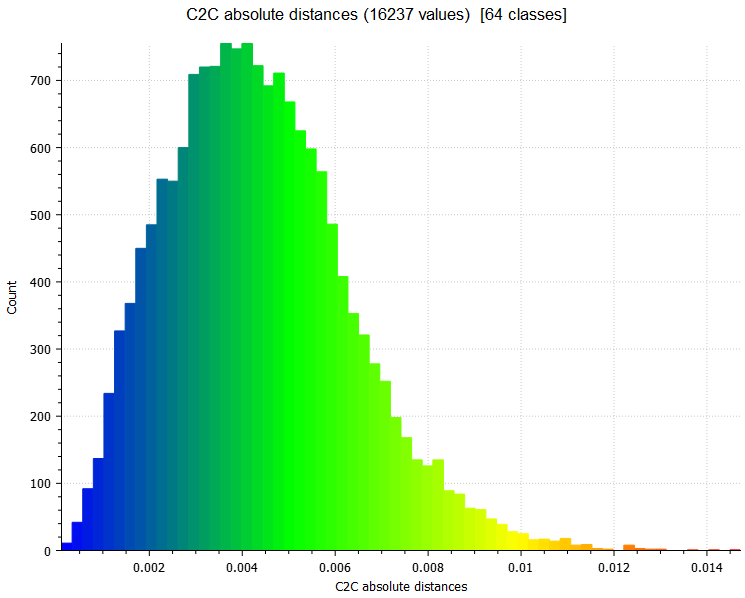

Figure 6. Histogram of the geometric comparison between station D and the ground truth. Source: The authors.

Station C against the ground truth (AB)

The accuracy of the far-intermediate cloud with the greatest angle (histogram of point distances in Figure 7):

Mean distance = 0.002897 metres

Standard deviation = 0.001245 metres

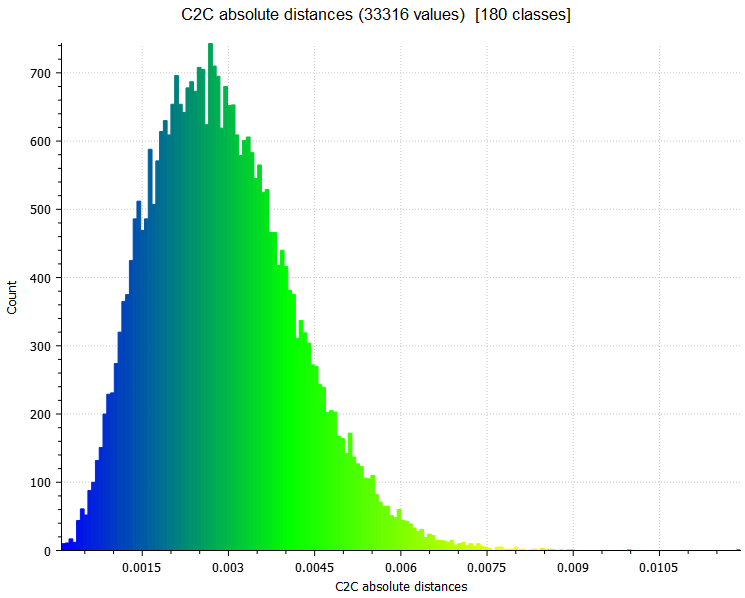

Figure 7. Histogram of the geometric comparison between station C and the ground truth. Source: The authors.

Stations D and C combined against the ground truth (AB)

The accuracy of the combination between stations D and C and the histogram of point distances (Figure 8) are given below:

Mean distance = 0.003370 metres

Standard deviation = 0.001658 metres

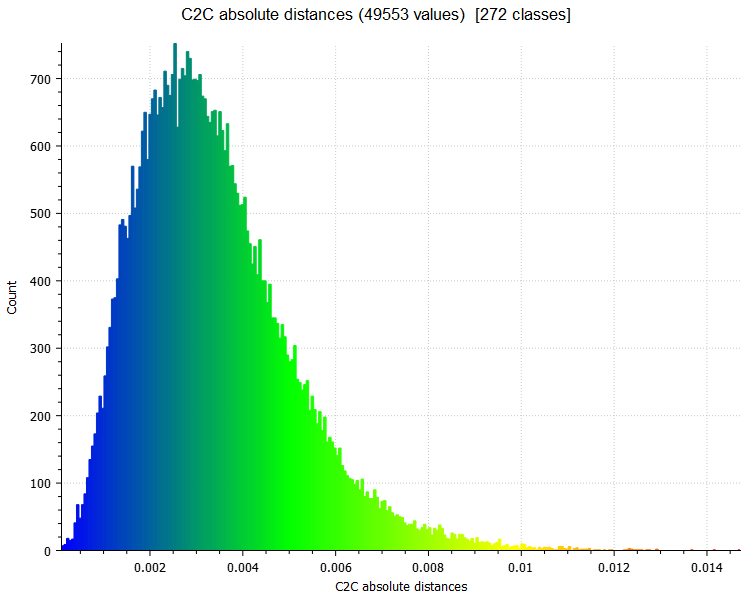

Figure 8. Histogram of the geometric comparison between the joint cloud from stations D and C and the ground truth. Source: The authors.

Given the standard deviation values from the geometric comparison between stations D, C, and their combination (D+C) against the ground truth (AB), it can be concluded that merging the datasets of both stations improves the accuracy of the point cloud from the most unfavourable station (D, also in terms of resolution), but does not enhance their accuracy as a joint point cloud.

Stations B and A against the ground truth (AB)

Before comparing stations B and A with the reference cloud, it is worth analysing their accuracy with each other (the histogram of their point deviation analysis is shown in Figure 9).

Mean distances = 0.001762 metres

Standard deviations = 0.000947 metres

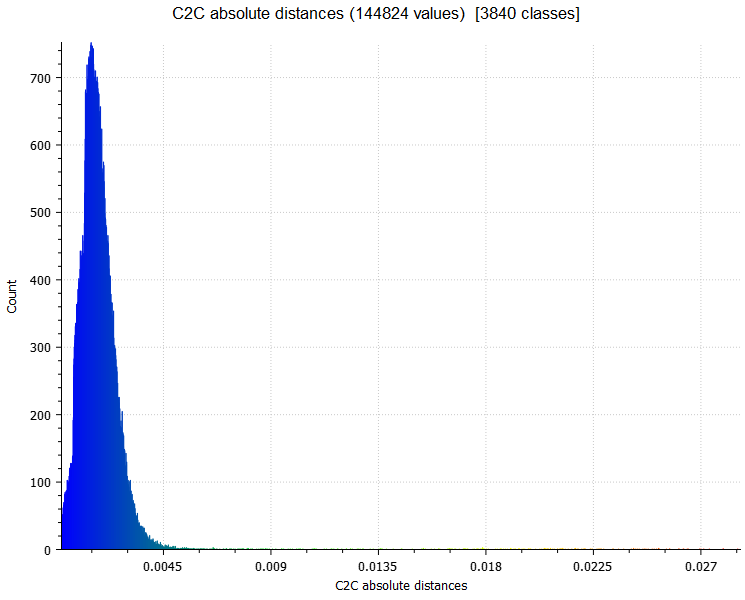

Figure 9. Histogram of the geometric comparison between stations B and A. Source: The authors.

In view of the accuracies of stations D and C against the reference dataset, stations B and A evidence a greater similarity with each other. Specifically: 59.41%, 39.18%, and 47.72% decrease against stations D, C, and C+D in mean distances and 51.49%, 23.94, and 42.88% decrease in standard deviation, respectively.

Besides, given the fact that stations A and B were used to build the ground truth by merging their clouds, it was expected that the comparison between them and the reference point cloud data (AB) yielded significantly low mean distances and high accuracies, as seen below:

Mean distances = 0.000000 metres (B); 0.000001 metres (A)

Standard deviations = 0.000030 metres (B); 0.000042 metres (A)

In these cases, given the great similarity between the clouds, the histograms are not provided. The datasets should be compared with the geometry of the reference 3D mesh (mesh AB Octree level 10, which will be validated below).

The analysis of station B against the reference mesh yielded the following data and histogram (Figure 10):

Mean distance = 0.000826 metres

Standard deviation = 0.000786 metres

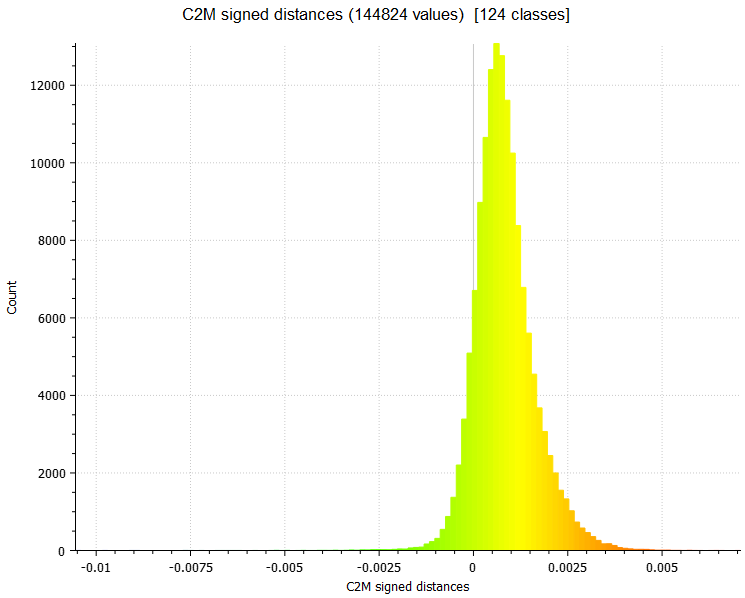

Figure 10. Histogram of the geometric comparison between station B and the reference mesh. Source: The authors.

The analysis of station A against the reference mesh yielded the following data and histogram (Figure 11):

Mean distance = 0.000225 metres

Standard deviation = 0.000400 metres

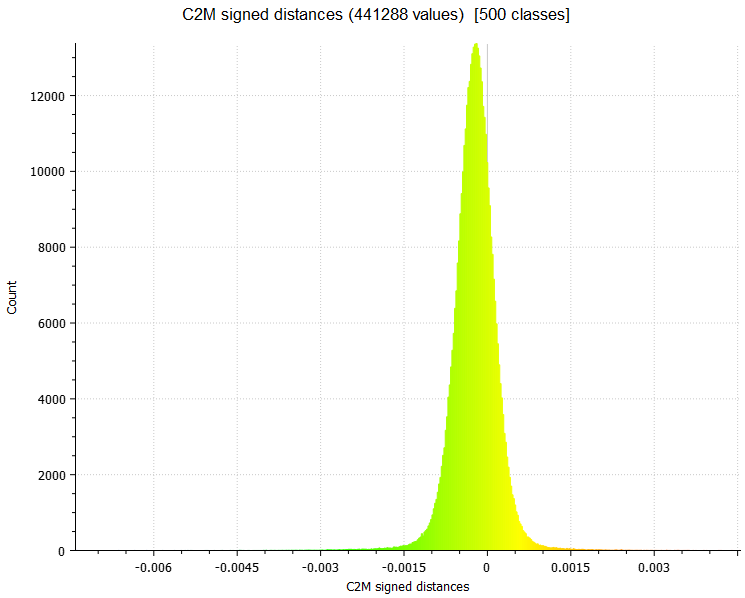

Figure 11. Histogram of the geometric comparison between station A and the reference mesh. Source: The authors.

The results of the analysis reveal that, due to the smaller distance of station A to the target wall and its slightly smaller angle of incidence, the cloud from A is twice as accurate as station B despite the fact that the scanning resolution was set at twice its value. The vertical scale in the histograms of stations B and A was constant to ease the recognition of the higher point accuracy in the latter.

3.1.2. Accuracies of 3D meshes

The 3D meshing algorithm was used on the reference cloud (AB) of the target wall to constitute a solid basis of geometrical data for the accuracy analysis of station clouds. Likewise, the chosen 3D meshing smoothening degree was validated for the purpose of modelling defects on heritage surfaces.

Figure 12 illustrates the 3D mesh created by selecting level 10 of the Octree Depth parameter in CloudCompare both with the TLS imaging colours and showing the graded point neighbouring density on its surface.

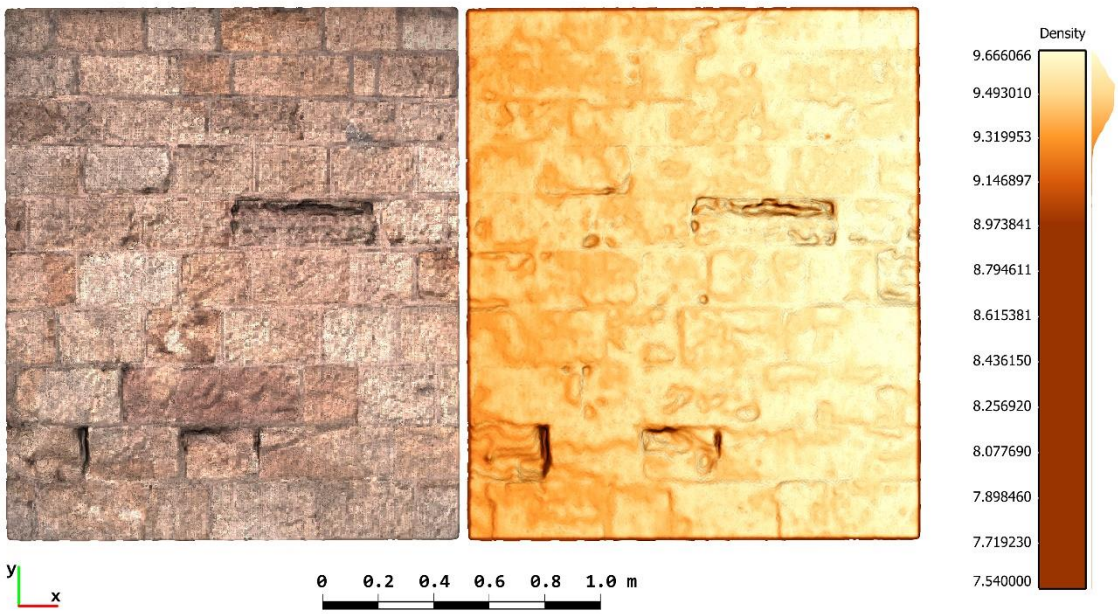

Figure 12. Octree level 10 3D mesh of the target wall in RGB and point neighbouring density visualisation modes. Elevation view. Source: The authors.

With a view to validating the meshing algorithm parameters to create the geometry in Figure 12, that 3D mesh was compared against a smoother mesh that benefits from a lower polygon count, i.e., a lower triangle resolution (bigger triangles), and, therefore, a lower file size.

Smooth mesh (AB, Octree level 9) against the reference mesh (AB, Octree level 10)

In qualitative terms, the relief of the 3D meshes of the target wall is clearly lower when applying level 9 to the smoothening degree (please see the three-part Figure 13), which has an impact on the representation of surface defects on heritage buildings.

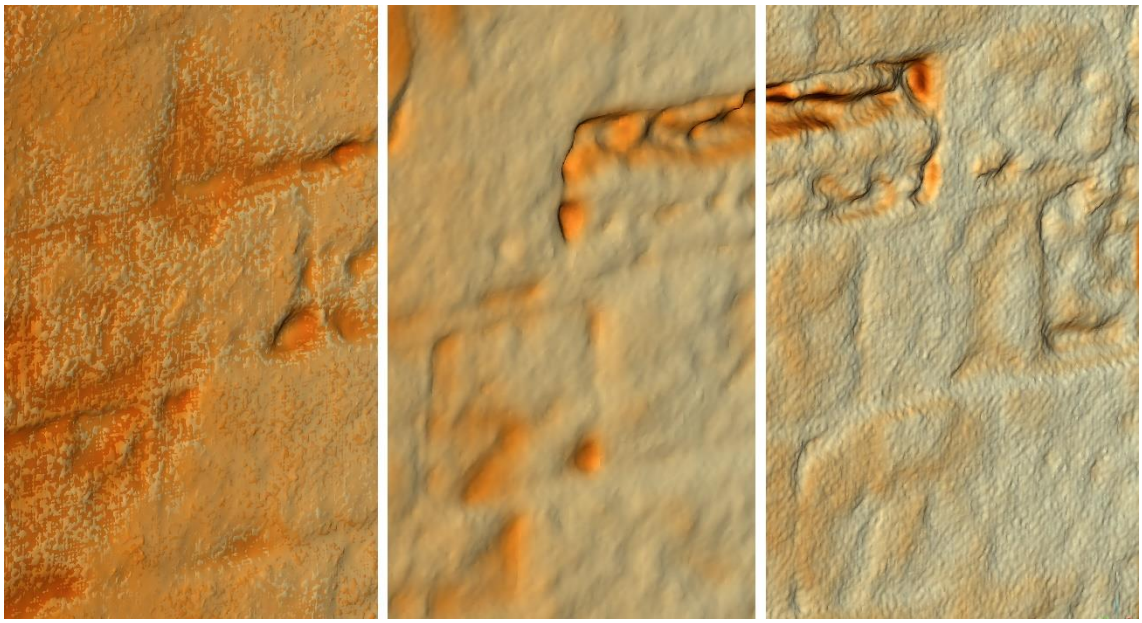

Figure 13. Detail of surface defects on 3D meshes: levels 9 and 10 overlapping (left); level 9 (centre); and level 10 (right). Source: The authors.

Focusing on quantitative data, the accuracy of 3D mesh level 9 against level 10 (reference mesh) is given below:

Mean distance = 0.000052 metres

Standard deviation = 0.000295 metres

Scalar field RMS = 0.000299847 metres

The histogram of their point deviation analysis is shown in Figure 14.

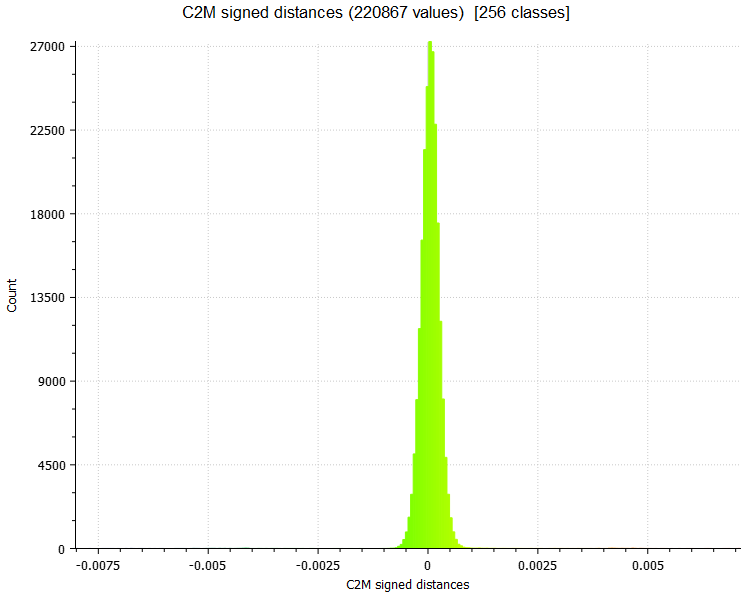

Figure 14. Histogram of the geometric comparison between 3D mesh level 9 and level 10 (reference mesh). Source: The authors.

Here, the 0.05 mm average distance between meshes and the approximately 0.3 mm errors could be accepted in favour of a lower polygon count. However, the global surface (area) and triangle surface (3D mesh resolution) of these meshes become essential aspects with regard to the reliability of the 3D representation. They can also be quantified so that the decision is based on accurate data.

Level 9:

Mesh Surface = 3.18227 m^2

Average triangle surface: 7.22781 x 10^{-6} m^2

Level 10:

Mesh Surface = 3.22211 m^2

Average triangle surface: 1.70902 x 10^{-6} m^2

In view of these data, there is an evident loss of geometry when smoothening the meshes. In particular, the level 9 mesh loses 1.24% of geometry, and its triangle resolution significantly decreases (greater triangle size, meaning a poorer geometry) by 76.35%.

Therefore, the 3D mesh generated using the Octree Depth level 10 was chosen as the reference mesh in the comparison for its ability to represent building surface deficiencies in a more accurate and representative way.

3.2. Limitations

In relation to the scan registration diagnostics from the TLS survey of Beeston Parish Church (Table 1), the reason for the alignment errors (RMSE values (from 2 to 3 mm) and average error of 4 mm in some cases) may have been the constant movement of the leaves and branches of the trees surrounding the temple. Nevertheless, as the comparison between stations A and B shows, their low alignment average error (1 mm) and great similarity (1.76 mm mean distance and 0.95 mm standard deviation) account for an accurate global registration, thus validating the accuracy analyses of point clouds and 3D meshes carried out.

The reason why there are no round distances and incidence angles between the stations and the target wall in Table 3 is that the experiment was not carried out under laboratory conditions but after an actual TLS survey at Beeston Parish Church for subsequent 3D modelling. Nonetheless, this does not translate into inaccurate analysis results.

4. Conclusions

3D laser scanning, particularly Terrestrial Laser Scanning (TLS), is commonly used to capture dimensions and develop 3D CAD models in buildings. In the field of cultural heritage, this technology is becoming crucial because of the need for a virtual record of buildings and to detect their surface wear and deterioration. Scientific research has demonstrated that exhaustive as-built modelling from 3D point cloud data allows for performing diverse accurate analyses of heritage buildings and sites. However, some issues in TLS surveying are the number and location of stations, the distance to the object, the point of view, and the resolution. These factors have a significant impact not only on the scanning and modelling accuracies but also on the intensity of the point cloud data for visual inspection and quantitative analyses.

This chapter investigates the accuracy and precision of TLS positioning and resolution to produce detailed models of damage features on heritage buildings. A sector of a masonry wall in an Anglican temple from the mid-19th century, St John the Baptist Beeston Parish Church in Nottingham, UK, was selected as a case study for this purpose.

This research sheds light on the accuracy that can be reached in a real TLS survey by combining different points of view and distances to target bodies. The results reveal that point cloud data of the building from a low-resolution scan station with a suitable angle to target can see its accuracy enhanced when combined with the cloud from another nearer station at a greater angle. Nonetheless, this research detected that the joint accuracy is still under that of the second station.

In addition, this chapter determined the suitable smoothening degree for a case study of such characteristics to model the geometrical alterations of the damage features on the target wall. The distortion from discretising (triangle-based 3D meshing) the 3D point cloud geometry was analysed and validated for the accuracy analysis of scan stations.

Finally, although it is expected that 3D scanning technologies will continue to improve, future research will delve into the analysis of additional samples of stations at different distances and incidence angles so that the scanning and modelling accuracies for geometrical alterations of surface pathologies at the millimetric scale are analysed under laboratory conditions for the digitisation and virtual reconstruction of heritage assets.

Acknowledgements

This research has been supported by funding for a post-doctoral researcher contract from the VI Plan Propio de Investigación y Transferencia of Universidad de Sevilla (reference VIPPIT-2020-II.5), Spain.

Additional support was granted by the 'Live Experiential and Digital Diversification – Nottingham' (LEADD:NG) project, part-funded by the European Union European Regional Development Fund (ERDF) (reference 08R20S04177) as part of the European Structural and Investment Funds Growth Programme 2014-2020, in partnership with Midlands Engine (The Government of the United Kingdom, HM Government), University of Nottingham, and Nottingham Trent University (UK).

The authors also wish to thank the School of Architecture, Design and the Built Environment at Nottingham Trent University for access to their TLS equipment and workstations for data processing.

Special thanks to Father Wayne Plimmer and St John the Baptist Beeston Parish Church for willingly granting access to their facilities.

References

Alkadri, M. F., Alam, S., Santosa, H., Yudono, A., & Beselly, S. M. (2022). Investigating Surface Fractures and Materials Behavior of Cultural Heritage Buildings Based on the Attribute Information of Point Clouds Stored in the TLS Dataset. *Remote Sensing*, *14*(2), 410. https://doi.org/10.3390/rs14020410

Antón, D., & Amaro-Mellado, J.-L. (2021). Engineering Graphics for Thermal Assessment: 3D Thermal Data Visualisation Based on Infrared Thermography, GIS and 3D Point Cloud Processing Software. *Symmetry*, *13*(2), 335. https://doi.org/10.3390/sym13020335

Antón, D., Carretero-Ayuso, M. J., Moyano-Campos, J., & Nieto-Julián, J. E. (2022). Laser Scanning Intensity Fingerprint: 3D Visualisation and Analysis of Building Surface Deficiencies. In D. Bienvenido-Huertas & J. Moyano-Campos (Eds.), *New Technologies in Building and Construction* (pp. 207–223). Springer Nature Singapore. https://doi.org/10.1007/978-981-19-1894-0_12

Antón, D., Medjdoub, B., Shrahily, R., & Moyano, J. (2018). Accuracy evaluation of the semi-automatic 3D modeling for historical building information models. *International Journal of Architectural Heritage*, *12*(5), 790–805. https://doi.org/10.1080/15583058.2017.1415391

Antón, D., Pineda, P., Medjdoub, B., & Iranzo, A. (2019). As-Built 3D Heritage City Modelling to Support Numerical Structural Analysis: Application to the Assessment of an Archaeological Remain. *Remote Sensing*, *11*(11), 1276.

https://doi.org/10.3390/rs11111276

Armesto-González, J., Riveiro-Rodríguez, B., González-Aguilera, D., & Rivas-Brea, M. T. (2010). Terrestrial laser scanning intensity data applied to damage detection for historical buildings. *Journal of Archaeological Science*, *37*(12), 3037–3047. https://doi.org/10.1016/j.jas.2010.06.031

Campiani, A., Lingle, A., & Lercari, N. (2019). Spatial analysis and heritage conservation: Leveraging 3-D data and GIS for monitoring earthen architecture. *Journal of Cultural Heritage*, *39*, 166–176. https://doi.org/10.1016/J.CULHER.2019.02.011

Chen, Z., Fan, R., Li, X., Dong, Z., Zhou, Z., Ye, G., & Chen, D. (2018). Accuracy improvement of imaging lidar based on time-correlated single-photon counting using three laser beams. *Optics Communications*, *429*, 175–179. https://doi.org/10.1016/j.optcom.2018.08.017

Dawson, P., Brink, J., Farrokhi, A., Jia, F., & Lichti, D. (2022). A method for detecting and monitoring changes to the Okotoks Erratic – "Big Rock" provincial historic site. *Journal of Cultural Heritage Management and Sustainable Development*, *ahead-of-p*(ahead-of-print). https://doi.org/10.1108/JCHMSD-10-2021-0183/FULL/PDF

Dayal, K. R., Tiwari, P. S., Sara, R., Pande, H., Kumar, A. S., Agrawal, S., & Srivastav, S. K. (2019). Diagnostic utilisation of ground based imaging and non-imaging sensors for digital documentation of heritage sites. *Digital Applications in Archaeology and Cultural Heritage*, *15*, e00117. https://doi.org/10.1016/j.daach.2019.e00117

Diara, F. (2022). HBIM Open Source: A Review. *ISPRS International Journal of Geo-Information*, *11*(9), 472. https://doi.org/10.3390/ijgi11090472

Disney, M., Burt, A., Calders, K., Schaaf, C., & Stovall, A. (2019). Innovations in Ground and Airborne Technologies as Reference and for Training and Validation: Terrestrial Laser Scanning (TLS). *Surveys in Geophysics*, *40*(4), 937–958. https://doi.org/10.1007/S10712-019-09527-X/FIGURES/9

Doğan, Y., & Yakar, M. (2018). GIS AND THREE-DIMENSIONAL MODELING FOR CULTURAL HERITAGES. *International Journal of Engineering and Geosciences*. https://doi.org/10.26833/ijeg.378257

Duchnowski, R., & Wyszkowska, P. (2022). Msplit Estimation Approach to Modeling Vertical Terrain Displacement from TLS Data Disturbed by Outliers. *Remote Sensing*, *14*(21), 5620. https://doi.org/10.3390/rs14215620

Girardeau-Montaut, D. (2015a). *Cloud-to-Cloud Distance*. https://www.cloudcompare.org/doc/wiki/index.php/Cloud-to-Cloud_Distance

Girardeau-Montaut, D. (2015b). *Cloud-to-Mesh Distance*. http://www.cloudcompare.org/doc/wiki/index.php?title=Cloud-to-Mesh_Distance

Girardeau-Montaut, D. (2016). CloudCompare: 3D point cloud and mesh processing software. In *Open Source Project*. http://www.danielgm.net/cc/

Haznedar, B., Bayraktar, R., Ozturk, A. E., & Arayici, Y. (2023). Implementing PointNet for point cloud segmentation in the heritage context. *Heritage Science*, *11*(1), 2. https://doi.org/10.1186/s40494-022-00844-w

Historic England. (1987). *Church of St John the Baptist, Non Civil Parish - 1263823*. Listing. https://historicengland.org.uk/listing/the-list/list-entry/1263823

Huang, J., Ran, S., Wei, W., & Yu, Q. (2022). Digital Integration of LiDAR System Implemented in

a Low-Cost FPGA. *Symmetry*, *14*(6), 1256. https://doi.org/10.3390/sym14061256

International Council on Monuments and Sites. (2004). *History of the Venice Charter*. https://www.icomos.org/venicecharter2004/history.pdf

International Council on Monuments and Sites. (2011). *The Athens Charter for the Restoration of Historic Monuments - 1931*. https://www.icomos.org/en/167-the-athens-charter-for-the-restoration-of-historic-monuments

Janeras, M., Roca, J., Gili, J. A., Pedraza, O., Magnusson, G., Núñez-Andrés, M. A., & Franklin, K. (2022). Using Mixed Reality for the Visualization and Dissemination of Complex 3D Models in Geosciences—Application to the Montserrat Massif (Spain). *Geosciences*, *12*(10), 370. https://doi.org/10.3390/geosciences12100370

Julin, A., Kurkela, M., Rantanen, T., Virtanen, J.-P., Maksimainen, M., Kukko, A., Kaartinen, H., Vaaja, M. T., Hyyppä, J., & Hyyppä, H. (2020). Evaluating the Quality of TLS Point Cloud Colorization. *Remote Sensing*, *12*(17), 2748. https://doi.org/10.3390/rs12172748

Kazhdan, M., & Hoppe, H. (2013). Screened poisson surface reconstruction. *ACM Transactions on Graphics*, *32*(3), 1–13. https://doi.org/10.1145/2487228.2487237

Klapa, P., & Gawronek, P. (2022). Synergy of Geospatial Data from TLS and UAV for Heritage Building Information Modeling (HBIM). *Remote Sensing*, *15*(1), 128. https://doi.org/10.3390/rs15010128

Leica Geosystems. (2012). *Leica ScanStation P20 – Industry's Best Performing Ultra-High Speed Scanner*. Scanners. http://w3.leica-geosystems.com/downloads123/hds/hds/ScanStation_P20/brochures-datasheet/Leica_ScanStation_P20_DAT_us.pdf

Leica Geosystems. (2019). *Leica Cyclone – 3D Point Cloud Processing Software* (9.4). HEXAGON. https://leica-geosystems.com/en-gb/products/laser-scanners/software/leica-cyclone

Lercari, N. (2019). Monitoring earthen archaeological heritage using multi-temporal terrestrial laser scanning and surface change detection. *Journal of Cultural Heritage*, *39*, 152–165. https://doi.org/10.1016/j.culher.2019.04.005

Lezzerini, M., Antonelli, F., Columbu, S., Gadducci, R., Marradi, A., Miriello, D., Parodi, L., Secchiari, L., & Lazzeri, A. (2016). Cultural Heritage Documentation and Conservation: Three-Dimensional (3D) Laser Scanning and Geographical Information System (GIS) Techniques for Thematic Mapping of Facade Stonework of St. Nicholas Church (Pisa, Italy). *International Journal of Architectural Heritage*, *10*(1), 9–19. https://doi.org/10.1080/15583058.2014.924605

Li, Y., Zhao, L., Chen, Y., Zhang, N., Fan, H., & Zhang, Z. (2023). 3D LiDAR and multi-technology collaboration for preservation of built heritage in China: A review. *International Journal of Applied Earth Observation and Geoinformation*, *116*, 103156. https://doi.org/10.1016/j.jag.2022.103156

Liao, K.-Y., Lu, M.-H., & Fan, Y.-C. (2022). 3D Point-cloud Segmentation System Based on AI Model. *2022 IEEE 4th Global Conference on Life Sciences and Technologies (LifeTech)*, 433–434. https://doi.org/10.1109/LifeTech53646.2022.9754862

Liu, K., & Boehm, J. (2015). Classification of Big Point Cloud Data using Cloud Computing. *The International Archives of the Photogrammetry, Remote Sensing and Spatial Information Sciences*, *XL-3/W3*, 553–557. https://doi.org/10.5194/isprsarchives-XL-3-W3-553-2015

Moyano, J., León, J., Nieto-Julián, J. E., & Bruno, S. (2021). Semantic interpretation of architectural and archaeological geometries: Point cloud segmentation for HBIM parameterisation. *Automation in Construction*, *130*, 103856. https://doi.org/10.1016/j.autcon.2021.103856

Nguyen, M. H., Yoon, S., Ju, S., Park, S., & Heo, J. (2022). B-EagleV: Visualization of Big Point Cloud Datasets in Civil Engineering Using a Distributed Computing Solution. *Journal of Computing in Civil Engineering*, *36*(3), 04022005. https://doi.org/10.1061/(ASCE)CP.1943-5487.0001021

Oytun, M., & Atasoy, G. (2022). Effect of Terrestrial Laser Scanning (TLS) parameters on the accuracy of crack measurement in building materials. *Automation in Construction*, *144*, 104590. https://doi.org/10.1016/j.autcon.2022.104590

Pajić, V., Govedarica, M., & Amović, M. (2018). Model of Point Cloud Data Management System in Big Data Paradigm. *ISPRS International Journal of Geo-Information*, *7*(7), 265. https://doi.org/10.3390/ijgi7070265

Patel, N., Parikh, K., & Patel, B. (2021). Bridge information modeling and AR using terrestrial laser scanner. *Reliability: Theory and Applications*, *16*(60), 17–23. https://doi.org/https://doi.org/10.24412/1932-2321-2021-160-17-23

Pepe, M., Costantino, D., Alfio, V. S., Restuccia, A. G., & Papalino, N. M. (2021). Scan to BIM for the digital management and representation in 3D GIS environment of cultural heritage site. *Journal of Cultural Heritage*, *50*, 115–125. https://doi.org/10.1016/j.culher.2021.05.006

Poux, F., Valembois, Q., Mattes, C., Kobbelt, L., & Billen, R. (2020). Initial User-Centered Design of a Virtual Reality Heritage System: Applications for Digital Tourism. *Remote Sensing*, *12*(16), 2583. https://doi.org/10.3390/rs12162583

Soudarissanane, S., Lindenbergh, R., Menenti, M., & Teunissen, P. (2011). Scanning geometry: Influencing factor on the quality of terrestrial laser scanning points. *ISPRS Journal of Photogrammetry and Remote Sensing*, *66*(4), 389–399. https://doi.org/10.1016/J.ISPRSJPRS.2011.01.005

Tan, K., & Cheng, X. (2017). Specular Reflection Effects Elimination in Terrestrial Laser Scanning Intensity Data Using Phong Model. *Remote Sensing*, *9*(8), 853. https://doi.org/10.3390/rs9080853

Tan, K., Zhang, W., Shen, F., & Cheng, X. (2018). Investigation of TLS Intensity Data and Distance Measurement Errors from Target Specular Reflections. *Remote Sensing*, *10*(7), 1077. https://doi.org/10.3390/rs10071077

The Southwell and Nottingham Church History Project. (2021). *Beeston St John the Baptist*. The Southwell & Nottingham Church History Project. https://southwellchurches.nottingham.ac.uk/beeston/hintro.php

United Nations Educational Scientific and Cultural Organization. (2019). *World Heritage*. World Heritage Centre. https://whc.unesco.org/en/about/

United Nations Educational Scientific and Cultural Organization (UNESCO). (1972). *The World Heritage Convention*. 17th General Conference of the United Nations Educational, Scientific and Cultural Organization. https://whc.unesco.org/en/conventiontext/

United Nations Educational Scientific and Cultural Organization (UNESCO). (2023a). *List of World Heritage in Danger*. World Heritage Centre. https://whc.unesco.org/en/danger/

United Nations Educational Scientific and Cultural Organization (UNESCO). (2023b). *World Heritage in Danger*. World Heritage Centre. https://whc.unesco.org/en/158

Xu, G., Pang, Y., Bai, Z., Wang, Y., & Lu, Z. (2021). A Fast Point Clouds Registration Algorithm for Laser Scanners. *Applied Sciences*, *11*(8), 3426. https://doi.org/10.3390/app11083426

Yang, S., Hou, M., & Li, S. (2023). Three-Dimensional Point Cloud Semantic Segmentation for Cultural Heritage: A Comprehensive Review. *Remote Sensing*, *15*(3), 548. https://doi.org/10.3390/rs15030548